Volume 30
Number 25
December 11, 1991

Inorganic Chemistry

Communications

Influence of Phosphine Conformation on the Structure and Stereodynamics of $Fe(CO)_4P(o\text{-tolyl})_3$ and $Cr(CO)_5P(o\text{-tolyl})_3$

As ancillary ligands in transition-metal complexes, phosphines provide great potential for control of structure and reactivity through variation of both steric and electronic properties. Though conformational isomerism in free triarylphosphines and related compounds has been extensively investigated,[1] much less is known about the stereodynamics of metal–phosphine complexes. As a contribution to the developing interest in this subject,[2] we describe here results on $Cr(CO)_5P(o\text{-tolyl})_3$ (**1**) and $Fe(CO)_4P(o\text{-tolyl})_3$ (**2**) which demonstrate that, for this sterically demanding phosphine, P–C rotation may be monitored by variable-temperature NMR techniques, that there is a clear relationship between phosphine conformation and the symmetry of the metal fragment, and, in **2**, that there is a novel dependence of intramolecular exchange within the trigonal bipyramid on phosphine conformation.

The solid-state structures of **1** and **2** (Figure 1)[3] reveal octahedral and trigonal-bipyramidal $M(CO)_nL$ frameworks, which, with the exception of elongated M–P bond lengths, differ little from their PPh_3 counterparts.[4] In contrast, the phosphine conformations differ significantly. While the iron complex exhibits an exo_3 propeller[5] in which the three methyl groups bisect the equatorial CO–Fe–CO angles, the chromium complex adopts an exo_2 conformation in which the endo ring is collinear with the Cr–P axis. Molecular modeling[6] suggests that the difference is steric in origin; superposition of an exo_3 conformation on a C_{4v} $Cr(CO)_5$ fragment or of an exo_2 conformation on a C_{3v} $Fe(CO)_4$ fragment[7] yields structures which are higher in energy by 36 and 5 kcal, respectively, due to increased methyl–carbonyl interactions.

The smaller energy difference for the iron complex may be noted, and while the ^{31}P NMR spectrum of **1** is temperature invariant, that of **2** is resolved into two resonances of unequal intensity at low temperature (Figure 2), which may be assigned

Table I. Rates and Activation Parameters

process	temp, K	rate const, s^{-1}	ΔG^*, kcal mol^{-1}
ring exch in **1**[a]	183	39	9.20
	193	135	9.25
	213	1500	9.23
	233	10500	9.24
	253	33000	9.50
	273	60000	9.96
$exo_2 \rightarrow exo_3$ exch in **2**[b]	213	45	10.71
	233	480	10.67
	253	2200	10.86
	273	10700	10.90
	293	33000	11.08
ax/eq CO exch in exo_3 **2**[c]	178	2	9.99
	198	50	9.89
	213	340	9.86
	233	3000	9.82
	253	24000	9.66
	293	470000	9.53
ax/eq CO exch in exo_2 **2**	178	6600	7.13
	198	40000	7.26
	213	300000	6.99

[a] $\Delta H^* = 8.5 \pm 0.5$ kcal mol^{-1}; $\Delta S^* = -3 \pm 2$ cal K^{-1} mol^{-1}. [b] $\Delta H^* = 9.5 \pm 0.5$ kcal mol^{-1}; $\Delta S^* = -5 \pm 2$ cal K^{-1} mol^{-1}. [c] $\Delta H^* = 10.7 \pm 0.2$ kcal mol^{-1}; $\Delta S^* = 4 \pm 1$ cal K^{-1} mol^{-1}.

(1) For reviews see: (a) Mislow, K. *Chemtracts: Org. Chem.* **1989**, *2*, 151. (b) Mislow, K. *Acc. Chem. Res.* **1976**, *9*, 26.

(2) For recent articles, see: (a) Davies, S. G.; Derome, A. E.; McNally, J. P. *J. Am. Chem. Soc.* **1991**, *113*, 2854. (b) Casey, C. P.; Whiteker, G. T.; Campana, C. F.; Powell, D. R. *Inorg. Chem.* **1990**, *29*, 3376. (c) Chudek, J. A.; Hunter, G.; MacKay, R. L.; Kremminghor, P.; Schlogl, K.; Weissensteiner, W. *J. Chem. Soc., Dalton Trans.* **1990**, 2001. (d) du Plooy, C. E.; Marcus, C. F.; Carlton, L.; Boeyens, J. C. A.; Coville, N. J. *Inorg. Chem.* **1989**, *28*, 3855.

(3) Data for complex **1** are as follows. Infrared (hexane): 2055, 1947, 1939 (sh), 1935 cm^{-1}. NMR: ^{31}P (CD_2Cl_2), 53.0 ppm; ^{13}CO (CD_2Cl_2), 217.0 (cis, J = 12.1 Hz), 221.1 ppm (trans, J = 7.3 Hz). Crystal data: monoclinic, space group $P2_1/n$, Z = 4, a = 10.774 Å, b = 14.951 Å, c = 14.687 Å, β = 91.45°. The structure was solved by direct methods (SHELX86)[9a] using 3795 independent observed data ($I > 3\sigma(I)$) and refined by full-matrix least-squares methods (SHELX76)[9b] to R = 0.0915 and R_w = 0.0980. Important bond lengths (Å) and angles (deg): Cr–P = 2.47, Cr–CO(cis) = 1.91 (av), Cr–CO(trans) = 1.85; P–Cr–CO(cis) = 92.5 (av), P–Cr–CO(trans) = 179, C–P–C = 104° (av). Data for complex **2** are as follows. Infrared (hexane): 2043, 1975, 1947 cm^{-1}. Crystal data: monoclinic, space group $P2_1/n$ (nonstandard $P2_1/c$), Z = 4, a = 10.188 Å, b = 10.429 Å, c = 21.755 Å, β = 99.79°. The structure was solved and refined as above using 2475 independent observed data ($I > 3\sigma(I)$) to R = 0.0520 and R_w = 0.0573. Important bond lengths (Å) and angles (deg): Fe–P = 2.31, Fe–CO(eq) = 1.77 (av), Fe–CO(ax) = 1.78 Å; P–Fe–CO(eq) = 90.7, P–Fe–CO(ax) = 179, CO(eq)–Fe–CO(eq) = 120 (av), C–P–C = 103° (av).

(4) (a) Plastas, H. J.; Stewart, J. M.; Grim, S. O. *Inorg. Chem.* **1973**, *12*, 265. (b) Riley, P. E.; Davis, R. E. *Inorg. Chem.* **1980**, *19*, 159.

(5) If a regular trigonal pyramid is constructed from the metal as apex and the three para ring carbons as the base, a proximal (exo) substituent will point away from the base while a distal (endo) substituent will point toward the base. The terms exo_3 and exo_2 define the number of proximal ortho methyl groups.

(6) CHEM-X, designed and distributed by Chemical Design Limited, Oxford, England. Minimization about conformationally mobile bonds (M–P, P–C, C–Me) using the default parameters reproduces closely the observed ground-state structures. The alternative higher energy structures for **1** and **2** were generated similarly but restricting the phosphine to either $C_3(exo_3)$ or $C_1(exo_2)$ symmetry, respectively. Energy differences between conformers are overestimated, since contributions to energy minimization through bond stretching and bending are neglected.

(7) The single a_1 vibration observed in solution at 2043 cm^{-1} is consistent with occupation of the axial position by the phosphine in both exo_2 and exo_3 conformations: Martin, L. R.; Einstein, F. W. B.; Pomeroy, R. K. *Inorg. Chem.* **1985**, *24*, 2777.

0020-1669/91/1330-4683$02.50/0

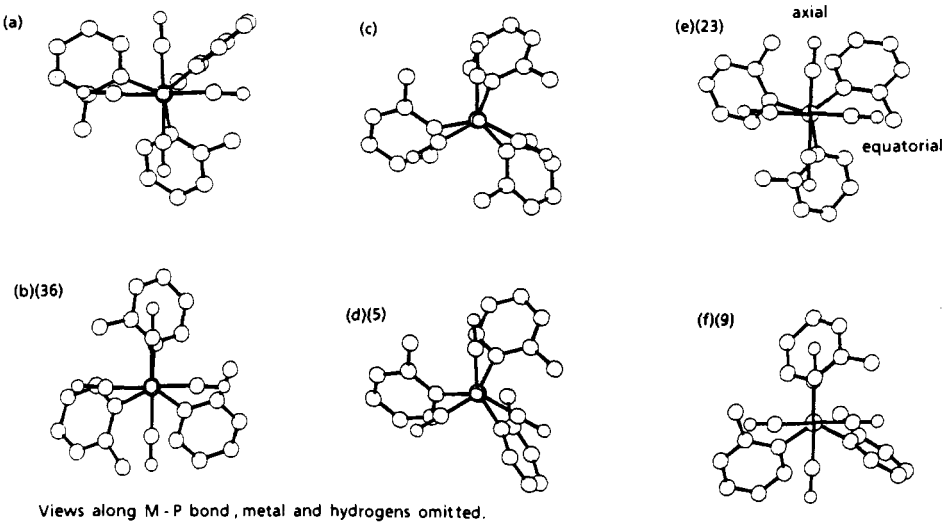

Views along M-P bond, metal and hydrogens omitted.

(a) complex (1), crystal structure. (b) complex (1), minimized exo$_3$ conformation. (c) complex (2), crystal structure. (d) complex (2), minimized exo$_2$ conformation. (e) complex (2), equatorial phosphine, minimized exo$_3$ conformation. (f) complex (2), equatorial phosphine, minimized exo$_2$ conformation. Numbers in parenthesis indicate energy in kcal relative to (a) or (c).

Figure 1. Lowest energy conformations of **1** and **2**.

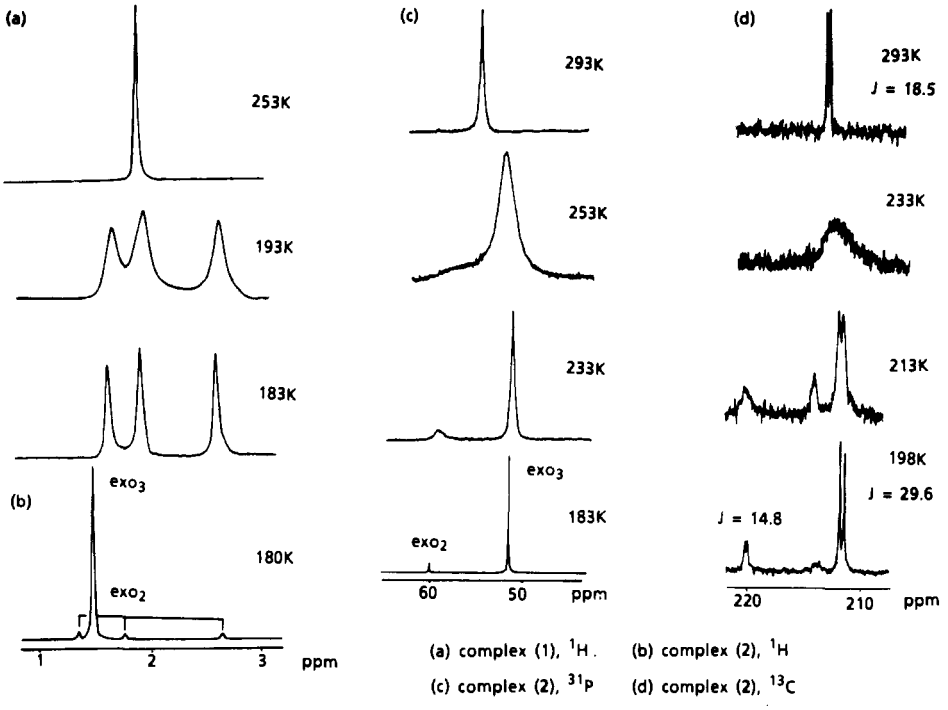

Figure 2. Variable-temperature NMR spectra (CD_2Cl_2 solvent).

to the exo$_3$ (major) and exo$_2$ (minor) isomers on the basis of the low-temperature ^{1}H NMR spectrum, which in the methyl region exhibits a single major resonance assignable to exo$_3$ together with three minor resonances of equal intensity assignable to exo$_2$. The ^{1}H NMR spectrum of **1** is resolved into only three resonances at low temperature, consistent with the presence of only exo$_2$ in solution. Line shape analysis yields the rates and activation parameters shown in Table I; the similarity may be noted and is consistent with the operation of a "two ring flip" mechanism,[1a] which results in both exo$_2$/exo$_3$ exchange and consequent ring exchange in the exo$_2$ conformer.

Of equal interest are the ^{13}C spectra of **2** (Figure 2), which reveal a dependence of intramolecular CO exchange on phosphine conformation. The room-temperature resonance is replaced at −75 °C by two resonances in the ratio 3:1, which are clearly assignable to the equatorial and axial carbonyls of the major exo$_3$ isomer, together with a single broadened resonance due to exo$_2$, which broadens further but remains unresolved at lower temperatures. As far as we are aware, this represents the first observation of a limiting low-temperature spectrum for a pentacoordinate Fe(CO)$_4$L complex containing a simple longitudinal ligand. Line shape analysis[8] shows the barrier to axial/equatorial exchange to be about 3 kcal lower in the exo$_2$ conformation. The origins again appear to be steric. Analysis of the Berry pseudorotation mechanism indicates that the equatorial Fe(CO)$_4$L isomer lies at or near the transition state. In a way which is reminiscent of the energy difference between the exo$_2$ and exo$_3$ conformations of **1**, modeling reveals a considerably lower energy for superposition of the C_1(exo$_2$) rather than C_3(exo$_3$) phosphine conformation on an equatorial C_{4v} Fe(CO)$_4$ fragment (Figure 1).[9] The similarity

(8) All line shape analyses were performed using the EXCHANGE program (R.E.D. McLung, University of Alberta). For **2** simulation assumes that the chemical shifts of the axial/equatorial resonances of the exo$_3$ and exo$_2$ conformations are identical. Note that J(P–CO$_{ax}$) and J(P–CO$_{eq}$) are of *opposite* sign; this has been demonstrated also for the cis/trans couplings in some M(CO)$_4$P$_2$ complexes (M = Mo, W): Colquhoun, I. J.; Grim, S. O.; McFarlane, W.; Mitchell, J. D.; Smith, P. H. *Inorg. Chem.* **1981**, *20*, 2516.

of the barrier for axial/equatorial exchange in the exo_3 conformation to the barrier for exo_2/exo_3 interconversion may be noted, and a correlated process cannot be discounted.

Restricted M–P bond rotation is evident only in a broadening of the cis carbonyl resonance of **1** at −90 °C. Thus, unlike PPh_3,[2a,c] phosphorus–carbon bond rotation in P(*o*-tolyl)$_3$ complexes appears to represent the process of highest energy. Preliminary results indicate that this is a general phenomenon and that since phosphine helicity is reversed via P–C rotation, variable-temperature NMR spectroscopy may be used to probe the diastereoisomeric relationship between phosphine helicity and other sources of molecular chirality.[11]

Supplementary Material Available: For **1** and **2**, Table 1S, containing crystallographic data, atomic coordinates, thermal parameters, bond lengths, and bond angles, and ORTEP diagrams, and Figure 1S, containing full calculated and experimental NMR spectra relevant to Table I of the text (36 pages); tables of structure factors (19 pages). Ordering information is given on any current masthead page.

(9) Crystal structure determinations of the few equatorial $Fe(CO)_4PR_3$ complexes which exist show a considerable distortion toward square pyramidal: (a) Cowley, A. H.; Kilduff, J. E.; Lasch, J. G.; Norman, N. C.; Pakulski, M.; Ando, F.; Wright, T. C. *J. Am. Chem. Soc.* **1983**, *105*, 7751. (b) Flynn, K. M.; Olmstead, M. M.; Power, P. P. *J. Am. Chem. Soc.* **1983**, *105*, 2085. (c) Sheldrick, W. S.; Morton, S.; Stelzer, O. *Z. Anorg. Allg. Chem.* **1981**, *475*, 232. (d) Forbes, E. J.; Jones, D. L.; Paxton, K.; Hamor, T. A. *J. Chem. Soc., Dalton Trans.* **1979**, 879. The structures of equatorial exo_2 and exo_3 $Fe(CO)_4P(o\text{-tolyl})_3$ were modeled using CO_{ax}–Fe–CO_{ax} and CO_{eq}–Fe–P angles of 172 and 117°, respectively.

(10) (a) Sheldrick, G. M. SHELX86, A Computer Program for Crystal Structure Determination. University of Gottingen, 1986. (b) Sheldrick, G. M. A Computer Program for Crystal Structure Determination. University of Cambridge, 1976.

(11) For example, both (*o*- and (*m*-$MeC_6H_4CO_2Me$)$Cr(CO)_2P(o\text{-tolyl})_3$ exist as 1:1 diastereoisomeric mixtures in solution[12] whereas (cyclohexadiene)$Fe(CO)_2P(o\text{-tolyl})_3$ exists as a single diastereoisomer in which helix reversal and iron–diene rotation may be correlated.[13]

(12) Howell, J. A. S.; Palin, M. G. Unpublished observations.

(13) Howell, J. A. S.; Palin, M. G.; Tirvengadum, M. C.; Cunningham, D.; McArdle, P.; Goldschmidt, Z.; Gottlieb, H. E. *J. Organomet. Chem.* **1991**, *413*, 269.

(14) To whom correspondence should be addressed.

Chemistry Department, University of Keele, Keele, Staffordshire ST5 5BG, Great Britain — **James A. S. Howell*,[14]**, **Michael G. Palin**

Chemistry Department, University College, Galway, Ireland — **Patrick McArdle**, **Desmond Cunningham**

Department of Chemistry, Bar Ilan University, Ramat Gan 52100, Israel — **Zeev Goldschmidt**, **Hugo E. Gottlieb**, **Dafna Hezroni-Langerman**

Received August 8, 1991

Crown Ether Encapsulation Effects upon Optical Electron-Transfer Energetics in a Symmetrical Mixed-Valence System

A key element in the energetics of many fluid-phase electron-transfer (ET) processes is the reorganization of solvent or other external environment.[1] Experimentally, the solvent energetic effects can be substantial—often comprising the majority of the observed barrier to activated electron transfer.[2,3] Recently we have begun to examine *molecular* aspects of solvent reorganization and have found that the largest fraction of the reorganization process (in an energetic sense) occurs within the first layer of solvent.[4] Given these findings, we reasoned that ET barriers, and ultimately kinetics, might be profoundly affected by systematic replacement of local solvent by micellar, polymer, protein, or other "encapsulating" environments. We wish to report here the results of a preliminary exploration of that concept; macrocyclic ethers (dibenzo crown species)[5,6] have been employed for encapsulation of an ammine-based mixed-valence complex, and ET energetics have been monitored via intervalence absorption measurements:[2,4,7]

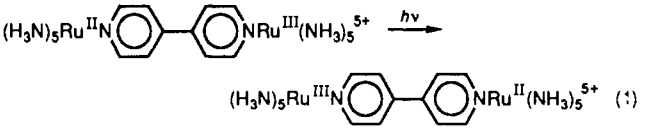

(1)

The key findings are first, that only small amounts of crown are required in order to achieve binding or encapsulation; second, that partial encapsulation has significant and unusual energetic consequences; but third, that complete encapsulation leads to only modest changes in total reorganization energy, at least in nitromethane as the reference solvent.

As suggested above, the overall optical barrier to intramolecular charge transfer can be evaluated by simple intervalence absorption energy measurements (eq 1). This energy (E_{op}) is known to be comprised of solvent reorganization (χ_s), vibrational reorganization (χ_i), redox asymmetry (ΔE) and electronic excited state ($\Delta E'$) terms:[2,4]

$$E_{op} = \chi_s + \chi_i + \Delta E + \Delta E' \qquad (2)$$

Our initial intent with crown encapsulation was chiefly to influence χ_s. As shown below, however, the largest energetic effect is a redox asymmetry effect.

Figure 1 shows a plot of the change in intervalence absorption energy (or optical barrier height) versus concentration of dibenzo-24-crown-8 (n = 0; see below) in nitromethane as solvent.[8]

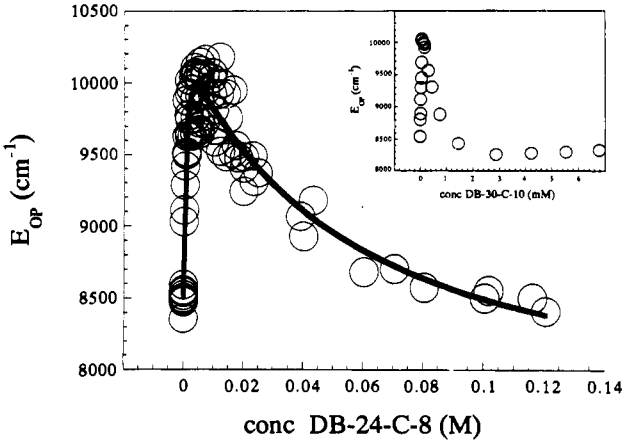

Figure 1. Optical intervalence absorption energy versus dibenzo-24-crown-8 concentration in nitromethane as solvent. Solid line represents the four-parameter fit described in the text. Measurement uncertainties (±100 cm^{-1}) are indicated by the diameters of the circles. Reproducibility is indicated by the spread in the points. (Note that the nine points clustered around 8500 ± 150 cm^{-1} were all measured at zero crown concentration.) The lowest nonzero DB-24-C-8 concentration was 3.6 × 10^{-4} M (see refs 8 and 14). Inset: data for dibenzo-30-crown-10.

(1) Marcus, R. A. *J. Chem. Phys.* **1965**, *45*, 679.

(2) (a) Creutz, C. *Prog. Inorg. Chem.* **1983**, *30*, 1. (b) Tom, G. M.; Creutz, C.; Taube, H. *J. Am. Chem. Soc.* **1974**, *96*, 7828.

(3) See, for example: Brown, G. M.; Sutin, N. S. *J. Am. Chem. Soc.* **1979**, *101*, 883.

(4) Blackbourn, R. L.; Hupp, J. T. *J. Phys. Chem.* **1988**, *92*, 2817.

(5) Pederson, C. J. *J. Am. Chem. Soc.* **1967**, *89*, 7017.

(6) (a) Colquhoun, H. M.; Stoddart, J. F.; Williams, D. J. *Angew. Chem., Int. Ed. Engl.* **1986**, *25*, 487. (b) Colquhoun, H. M.; Lewis, D. F.; Stoddart, J. F.; Williams, D. J. *J. Chem. Soc., Dalton Trans.* **1983**, 607. (c) Colquhoun, H. M.; Stoddart, J. F. *J. Chem. Soc., Chem. Commun.* **1981**, 612. (d) Colquhoun, H. M.; Stoddart, J. F.; Williams, D. J.; Wolstenholm, J. B.; Zarzycki, R. *Angew. Chem., Int. Ed. Engl.* **1981**, *20*, 1051.

(7) Hush, N. S. *Prog. Inorg. Chem.* **1967**, *8*, 391.

0020-1669/91/1330-4685$02.50/0